Contribution of Individual Tryptophan Residues to the Fluorescence Spectrum of Native and Denatured Forms of Human Carbonic Anhydrase II†

Lars-Göran Mårtensson,‡ Per Jonasson,‡ Per-Ola Freskgård,§ Magdalena Svensson,§ Uno Carlsson,§ and Bengt-Harald Jonsson*,‡

Department of Biochemistry, Umeå University, S-90187 Umeå, Sweden, and IFM-Department of Chemistry, Linköping University, S-581 83 Linköping, Sweden

Received May 9, 1994; Revised Manuscript Received September 26, 1994®

ABSTRACT: Measurements were made of fluorescence spectra produced by pseudo-wild-type human carbonic anhydrase II and mutants in which the tryptophan residues had been replaced by phenylalanine or cysteine residues. 2D NMR spectra of ^{15}N-labeled proteins indicated that the mutations had essentially no long range effects on structure and that the pertubations of structure in the vicinity of the mutated Trp were small. The individual contributions of the seven tryptophan residues were deduced from measurements on native proteins and on proteins subjected to various denaturing conditions. Trp97 and Trp245 are the major fluorescence emitters in the native state, contributing 52% and 38%, respectively, to the total fluorescence intensity. Comparisons of the fluorescence yield of pseudo-wild-type human carbonic anhydrase II and mutant proteins also indicate net energy transfer from Trp16 to Trp5 and from Trp192 to Trp209. The fluorescence from Trp5 is efficiently quenched by His64. In addition, acrylamide quenching of fluorescence was used to probe the environment of tryptophans in proteins incubated in 0, 1.5, and 5 M guanidine hydrochloride. The results indicate that the part of the native protein that corresponds to β-strands 3−7 forms a compact core in a molten globule intermediate.

Aromatic amino acids, especially tryptophans, have often been used as intrinsic probes to monitor the unfolding, refolding, and stability of proteins. This procedure is based on the knowledge that the spectral properties of these amino acids, when measured as UV absorption or fluorescence, vary according to whether the residue is situated in an apolar or a polar environment. Hence, the use of tryptophan side chains as probes will indicate changes in structure during, for example, unfolding.

The present method for fluorescence monitoring of unfolding has, among others, the following advantages: it requires only small amounts of samples, and it has a high signal to noise ratio. On the other hand, most proteins contain more than one tryptophan, and it is often difficult to sort out the contributions made by the individual tryptophans. To circumvent the problem of analyzing the individual contributions of fluorescence intensity, other less fluorescent residues can be substituted for the tryptophans, as described by Loewenthal et al. (1991) for barnase, a small ribonuclease. Smith et al. (1991) used another approach taking advantage of the fluorescence properties of tryptophans in combination with site-directed mutagenesis, i.e., tryptophans were introduced into various parts of the protein lactate dehydrogenase as reporter groups.

In the present study, we used human carbonic anhydrase II (HCA II,[1] EC 4.2.1.1), which is a monomeric zinc-containing enzyme with a molecular weight of 29 300 and 259 amino acid residues (Henderson et al., 1976). Several authors have studied the unfolding and refolding of carbonic anhydrase analyzing different physical parameters, such as UV absorbance, circular dichroism, and fluorescence (Carlsson et al., 1973; McCoy et al., 1980; Henkens et al., 1982).

HCA II contains seven tryptophans (Figure 1), six of which are evolutionarily conserved in the cytosolic isoenzymes of mammalian species (Hewett-Emmett et al., 1984). The measurement of absorbance to follow the denaturation of HCA II in various GuHCl concentrations reveals two transitions of almost equal amplitude; the first of these (at low GuHCl concentrations) coincides with the transition observed for the loss of CO_2 activity. The main purpose of this study was to investigate protein unfolding by use of the spectral properties of Trp residues. The changes in spectra when the Trp residues evolve from a buried (mostly apolar) to an exposed (polar) environment are reflected in the F_{332}/F_{352} ratio (Banik et al., 1992). Since, as noted above, the fluorescence spectrum from a tryptophan residue reports about the chemical properties of its surrounding, it is interesting to assess the contributions from each particular tryptophan to the composite spectrum of the protein. Therefore, we made a series of mutants that will be referred to in the following text as tryptophan mutants. The single mutant C206S, which lacks cysteines, was used as a reference protein and is called pseudo-wild-type (pwt). The strategy for site-directed mutagenesis involved mutating tryptophan residues (i) to the less fluorescent phenylalanine residues (W5F, W5F/W16F, W16F, W192F, and W209F) and (ii) to cysteinyl residues (W97C, W123C, and W245C). The Cys

† This work was supported by grants from the "Swedish National board for Technical Development" (U.C. and B.-H.J.), the "Swedish Natural Science Research Council" (U.C. and B-H.J.), and the "Sven och Lilly Lawskis fond" (P.-O.F. and L.-G.M.).

* Author to whom correspondence should be addressed.

‡ Umeå University.

§ Linköping University.

® Abstract published in *Advance ACS Abstracts,* December 15, 1994.

[1] Abbreviations: GuHCl, guanidine hydrochloride; HCA II, human carbonic anhydrase II; IPTG, isopropyl β-thioglactopyranoside; pwt, pseudo-wild-type; PCR, polymerase chain reaction; ssDNA, single-stranded DNA.

0006-2960/95/0434-1011$09.00/0

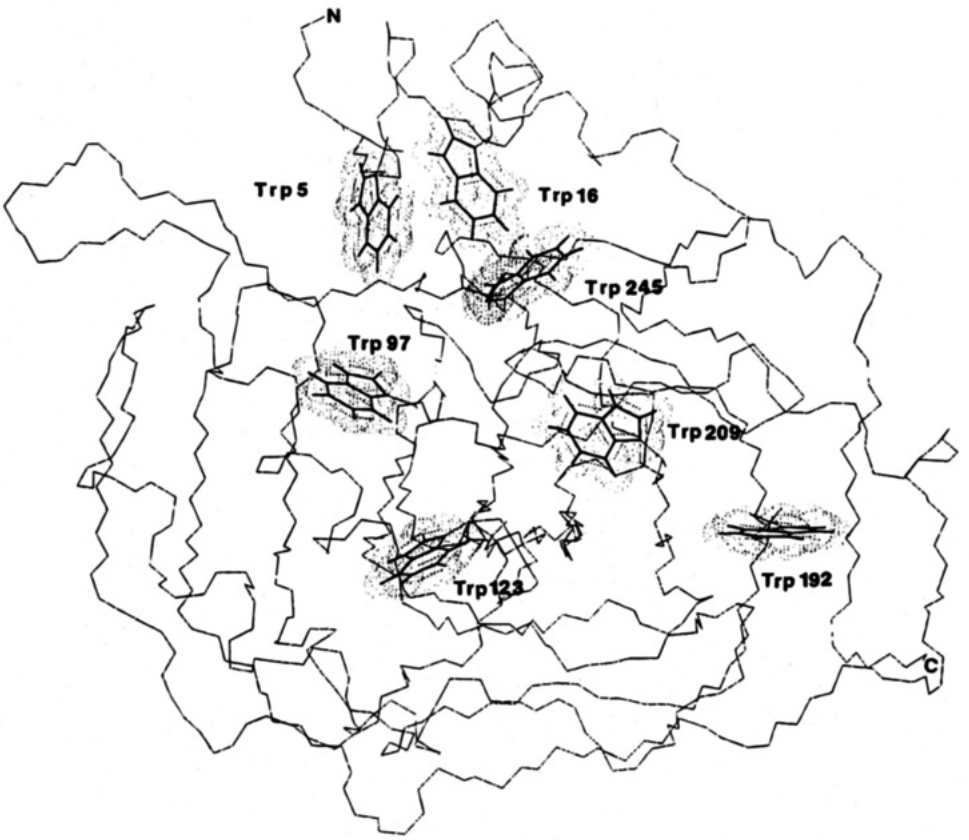

FIGURE 1: View of the polypeptide backbone of human carbonic anhydrase II, including the side chains of the seven tryptophan residues [from coordinates kindly provided by Håkansson et al. (1992)].

mutants were also used to introduce different thiol-specific reagents as extrinsic probes in a study presented elsewhere. This repertoire of mutants was characterized by measuring the fluorescence spectra of the mutant proteins under various denaturing conditions. Fluorescence quenching by acrylamide was also monitored.

MATERIALS AND METHODS

Chemicals. Guanidine hydrochloride (sequential grade) was purchased from Pierce. Concentrations of GuHCl were confirmed by measuring the index of refraction (Nozaki, 1972). Isopropyl β-thiogalactopyranoside (IPTG) was obtained from Promega. Acrylamide from Bio-Rad was electrophoresis grade. All other chemicals were reagent grade.

Spectrophotometers. Light absorbance was measured on either a Perkin-Elmer 320 or a Hitachi U2000 spectrophotometer. Fluorescence was measured on the following spectrofluorophotometers: Shimadzu RF-5000, Perkin-Elmer 204, and Hitachi F4500. NMR measurements were performed on a Bruker AMX2-500.

Mutagenesis. In vitro site-directed mutagenesis was performed essentially according to the method of Kunkel (1985), which is based on the production of single-stranded DNA (ssDNA) in host cells that are deficient in the enzymes dUTPase (*dut*$^-$) and uracil *N*-glucosylase (*ung*$^-$). Mutants were obtained by *in vitro* second-strand synthesis from oligonucleotides containing mismatches, followed by transformation of *Escherichia coli* (*ung*$^+$,*dut*$^+$), and were identified by direct sequenching of the plasmid DNA. Usually, 50% or more of the clones contained the desired mutant plasmid. Uracil-containing ssDNA was obtained from the expression plasmid pACA (Nair et al., 1991), harbored in *C. coli* strain CJ236 (*dut*$^-$,*ung*$^-$), after infection with the helper phage M13K07. The plasmid pACA contains the gene for human carbonic anhydrase II, and this gene is under the regulatory control of T7 RNA polymerase promoter; the plasmid also exhibits an F1 origin of replication (which allows production of ssDNA) and a gene for ampicillin resistance. W192F was the only mutant that could not be isolated by the procedure described, and it was therefore constructed using a method based on the polymerase chain reaction (PCR), as described by Hemsley et al. (1989); this work was done on a Perkin-Elmer Cetus thermal cycler.

A plasmid containing the mutation was used to transfect *E. coli* BL21(DE3) (Studier & Moffat, 1986). The mutation and the complete coding region were checked by plasmid sequencing before the clone was used for protein production; this was done to ensure that no spontaneous mutations had occurred. All sequencing was performed according to the chain termination method (Sanger et al., 1977).

Protein Production and Purification. E. coli BL21(DE3) harboring the mutant plasmid was grown in 2× Luria broth, 0.5 mM $ZnSO_4$, and 50 μg/mL ampicillin at 23 °C. Protein production was initiated by adding IPTG to a final concentration of 0.5 mM, at a cell density corresponding to OD^{660} = 0.5, and then allowing the cells to grow for 6−12 h. Uniformly ^{15}N-labeled protein variants were produced by use of conditions similar to those described, except that the cells were allowed to grow in a defined medium consisting of 0.5 g/L $^{15}NH_4Cl$, 0.5 g/L NaCl, 6 g/L Na_2HPO_4, 3 g/L KH_2PO_4, 4 g/L glucose, 0.5 mM $ZnSO_4$, and 50 mg/L ampicillin. All enzyme variants were purified to homogeneity in one step by use of affinity chromatography (Khalifah et al., 1977),

and the purified enzymes were examined by SDS−PAGE. Protein concentrations were determined from the absorbance at 280 nm and the proper extinction coefficients. For the pwt, the extinction coefficient at 280 nm is taken to be the same as that of the wild-type enzyme: 54 800 M^{-1} cm^{-1} (Nyman & Lindskog, 1964). The A_{280} values were measured for the tryptophan mutants in the native state, as well as denatured in 6 M GuHCl, and the corresponding extinction coefficients were calculated (Gill & von Hippel, 1989). The following values were obtained: W5F, 50 500 M^{-1} cm^{-1}; W5F/W16F, 43 800 M^{-1} cm^{-1}; W16F, 49 000 M^{-1} cm^{-1}; W97C, 49 000 M^{-1} cm^{-1}; W123C, 49 500 M^{-1} cm^{-1}; W192F, 49 800 M^{-1} cm^{-1}; W209F, 48 300 M^{-1} cm^{-1}; W245C, 50 400 M^{-1} cm^{-1}.

Activity Measurements. The CO_2 hydration activity exhibited by the various mutants when the GuHCl concentration was increased was measured as described previously (Mårtensson et al., 1992). The relative activities of the various mutants are reported in relation to the activity of the pwt, which is considered to be 100%.

Fluorescence Measurements. Fluorescence emission spectra were recorded with excitation at 295 nm. All measurements were made in 1-cm quartz cells; the sample compartment was maintained at 23 °C, and the pH was kept at 7.5 using 0.1 M Tris−SO_4. Data were corrected so that the differences in absorbance at 295 nm between the different mutants should not affect the total fluorescence intensity. A correction factor, antilog ΔABS, was applied, in which ΔABS is the difference in absorbance between the pwt and the particular mutant protein at a concentration of 0.85 μM in a cell with 1-cm path length (Eftink & Ghiron, 1976). Since the absorbance of the protein solutions is very low at this concentration, these corrections were less than 0.9%.

Acrylamide Quenching of Fluorescence. Samples containing 0.85 μM protein and 0.1 M Tris−SO_4 (pH 7.5) were equilibrated at three different GuHCl concentrations (0, 1.5, and 5.0 M) for 24 h. The fluorescence of the protein was quenched by the progressive addition of small aliquots of an 8 M acrylamide stock solution to a maximal concentration of 660 mM acrylamide. The Trp residues were excited at 295 nm, and quenching of the fluorescence was measured at the emission maximum. After corrections for dilution of the sample and for inner filter effects caused by acrylamide absorption ($\epsilon_{295} = 0.25$ M^{-1} cm^{-1}), the quenching data were fitted to the modified form of the Stern−Volmer relationship (Eftink & Ghiron, 1976):

$$F_0/F = (1 + K_{sv}[Q]) \exp(V[Q])$$

where F_0 and F are the fluorescence intensities in the absence and presence of the quencher, respectively, [Q] is the concentrationof quencher, K_{sv} is the dynamic quenching constant, and V is the static quenching constant.

Stability Measurements. The stability of the enzyme was measured in two sets of experiments in which the denaturation by GuHCl was monitored by recording intrinsic fluorescence or by recording the UV absorbances at 292 and 260 nm. Both sets of experiments were started by incubating the enzyme in various concentrations (0−5 M) of GuHCl buffered with 0.1 M Tris−SO_4 (pH 7.5) at 23 °C for 24 h. Enzyme concentrations of 0.85 and 8.5 μM were used when the denaturation was to be measured as fluorescence and UV absorbance, respectively. The fluorescence intensity at various concentrations of GuHCl was plotted as the fluorescence intensity (F_{332}) at the emission wavelength 332 nm and also as the ratio F_{332}/F_{352} between the fluorescence intensities at 332 and 352 nm.

UV absorbance was measured in a double-beam spectrophotometer in which the reference and the sample contained identical concentrations of buffer and denaturant. To compensate for variations in enzyme concentration during the spectrophotometric measurement, the A_{292}/A_{260} ratio was determined for each sample, since A_{260} has been shown to be unaffected by complete denaturation (Edsall et al., 1966) and is therefore a suitable internal standard (Mårtensson et al., 1992).

NMR Measurements. The HSQC (homonuclear single-quantum coherence) NMR experiments were performed essentially as described by Bodenhausen and Ruben (1980). The H_2O peak was suppressed by a low-power presaturation pulse during the 1.2-s relaxation delay. All spectra were recorded with identical t_1 (10 ms) and t_2 (123 ms) acquisition times, and the total measuring time was 30 min for each spectrum. To make sample conditions as similar as possible, all protein variants were dialyzed together against distilled H_2O in a single vessel, whereafter they were freeze-dried. Samples were 1−1.5 mM, uniformly ^{15}N-labeled proteins in 50 mM sodium phosphate buffer at pH 6.4, containing 0.25 mM NaN_3 at 30 °C in a 9:1 H_2O/D_2O solution.

Data Analysis. Since the course of enzyme unfolding is sequential, the data summarized in Table 1 were obtained from a nonlinear least-squares analysis (Garvey & Matthews, 1989) of a three-state model, including a native state (N), an intermediate state (I), and an unfolded state (U) (Mårtensson et al., 1993).

Molecular Graphics. The X-ray structure of HCA II was analyzed on a Silicon Graphics workstation (IRIS INDIGO XS24), using the program INSIGHT II (BIOSYM, Inc.), and the coordinates were kindly provided by Håkansson et al. (1992).

Table 1: Protein Stability toward GuHCl Denaturation of the Pseudo-Wild Type and the Seven Tryptophan Mutants of HCA II Investigated by Three Independent Parameters and Presented as Midpoint Concentrations (C_m) of Denaturation[a]

enzyme variant	C_{mNI} (M) enzymic activity	C_{mNI} (M) A_{292}/A_{260}	C_{mIU} (M) A_{292}/A_{260}	relative activity
pwt	0.97 ± 0.07	0.97 ± 0.07	2.1 ± 0.3	100
W5F	0.69 ± 0.09	0.69 ± 0.09	2.0 ± 0.4	86
W16F	0.39 ± 0.03	0.39 ± 0.04	2.0 ± 0.3	43
W97C	0.37 ± 0.02	0.47 ± 0.06	1.9 ± 0.3	51
W123C	0.65 ± 0.12	0.65 ± 0.09	2.0 ± 0.6	56
W192F	0.85 ± 0.08	0.86 ± 0.09	2.0 ± 0.3	74
W209F	0.62 ± 0.05	0.62 ± 0.06	2.0 ± 0.4	34
W245C	0.60 ± 0.07	0.60 ± 0.10	2.1 ± 0.4	100

[a] C_{mNI} and C_{mIU} represent the transition midpoint concentrations (GuHCl) for the transition from native to intermediate and from intermediate to denatured enzyme, respectively. The errors included in the table are standard deviations.

RESULTS

Effect of Mutations on the Stability and Activity of the Protein. The stability for each mutant as a function of GuHCl concentration was investigated by considering two independent properties: absorbance of UV light at 292 nm by tryptophan residues, plotted as the ratio A_{292}/A_{260}, and enzymic CO_2 hydration activity. The data obtained from

the different denaturation curves are summarized in Table 1. The ratio A_{295}/A_{260} shows that the pwt and all investigated mutants unfold in two, well-separated transitions when the GuHCl concentration is raised from 0 to 5 M, indicating the existence of a stable intermediate state (I) with residual structure (Mårtensson et al., 1993). Comparison of transition midpoint values (C_m) calculated from the results of the two different experiments shows that the values do not depend on the physical parameter that was measured. For the first transition (at low GuHCl concentrations), recorded as absorbance, and the single transition from inactivation of CO_2 hydration, the midpoint varies from 0.3 to 0.9 M GuHCl for the different mutants, while the value for the pwt is close to 1.0 M. The second transition (at high GuHCl concentrations) seems to be less affected by the mutations, since the relative variation in C_m values is smaller. The enzymatic activities of the mutants decrease by 14% to 66% for the different mutants. This drop in activity is roughly equivalent to an increase in activation energy of 1 kcal/mol (or less), which in turn may correspond to the loss of one elementary interaction such as a hydrogen bond. The relative CO_2 hydration activity for the most affected single mutant, W209F, was 34%. Since Trp209 is located in the active site region, where the closest distance to the catalytic Zn(II) ion is 5.3 Å, the lowered enzymatic activity may originate from the mutation *per se*. All mutant variants can be expressed in a high yield of 50−100 mg of purified protein per liter of growth medium.

Characterization of the Structural Integrity of Mutants by HSQC-NMR. For a meaningful interpretation of the fluorescence studies, it is important to demonstrate whether or not significant pertubations were introduced by the mutations. We found it especially important to investigate whether a mutation at one Trp would affect the environment of the other Trp. For this reason, we have produced ^{15}N-labeled proteins including the pwt and six of the mutant proteins (W5F, W16F, W97C, W123C, W192F, and W209F). Since the Trp indole ring contains an NH group, these ^{15}N-labeled proteins contain probes that, in HSQC-NMR spectra, report not only from all peptide NHs but also directly from the Trp side chains. The chemical shifts of these nitrogens and their corresponding protons are extremely sensitive to the chemical environment. A comparison of all recorded NMR spectra made it possible to identify peaks that correspond to the NH group in the indole rings of Trp5, Trp123, Trp192, and Trp209 and a tentative assignment of Trp97. These assignments are shown in the aromatic region of the HSQC-NMR spectra of pwt in Figure 2, which also includes spectra of the W97C and W192F mutants. We could not assign a peak to Trp16, and an analysis of the crystallographic structure showed that the NH of the Trp16 indole is subjected to strong ring currents from the neighboring Tyr7. Since the indole NH is positioned perpendicular to the Tyr7 ring, the peak is most probably shifted into the main envelope of peaks from the peptide NH groups, a fact that makes assignment less straightforward. Therefore, we could not draw any firm conclusions about the environment of Trp16 in the different mutants.

However, the assignments made it possible to directly evaluate the structural consequences of the mutations for the environments of all five assigned Trp's. The results show the following: (i) The mutations W5F, W123C, W192F, and W209F do not alter the structure at any of the assigned Trp's, because their corresponding peaks are not shifted at all. (ii) The mutation W16F does not at all affect the structure at Trp97, Trp123, and Trp192. The Trp209 peak is shifted 0.02 ppm in the ^1H dimension and 0.3 ppm in the ^{15}N dimension, indicating only small changes in local structure. As was expected for Trp5 (which normally makes van der Waals contacts with the mutated Trp16), the environment is altered, which is reflected in that the Trp5 peak has now shifted by 0.2 and 0.9 ppm in the ^1H and ^{15}N dimensions, respectively. (iii) The mutation W97C does not affect the structures at Trp123 and Trp192, while the structure at Trp5 is slightly altered since the corresponding peak has shifted by 0.05 and 0.1 ppm in ^1H and ^{15}N dimensions, respectively, and for Trp209 we observe a complex shift pattern that is not easily interpreted. Comparisons of the spectra, from all of the proteins, in the peptide NH region show that, with the exception of a few peaks in each spectra, they are remarkably similar, which strongly indicates that the secondary and tertiary structures of the mutant proteins and pwt are almost identical.

We conclude from the NMR results that, in general, the Trp mutations have essentially no long range effects on structure and in most cases only minor effects on the local structure around the mutation as well. Thus, the discussion of the fluorescence data for these mutants rests on a solid structural basis. Additional evidence for the structural integrity of these mutants can be found in a paper by Freskgård et al. (1994) in which results from CD measurements on these mutants are presented. Notably, near-UV CD spectra of the mutants indicate that the structure around the remaining Trp is essentially unaffected by mutation at another Trp.

Denaturation Measured by Fluorescence. A plot of the ratio between the fluorescence emission intensities at 332 and 352 nm gave rise to smooth transition curves, indicating two cooperative unfolding events for all mutants (Figure 3). It should be noted that the ratio F_{332}/F_{352} is not necessarily linearly correlated to concentrations of various forms of the protein. However, by calculating F_{332}/F_{352}, factors (such as concentration differences) that affect the whole spectrum similarly are effectively filtered off. Therefore, the ratio in a clear way shows the shift of fluorescence toward longer wavelengths as the proteins are subjected to higher concentrations of GuHCl (Banik et al., 1992). Apparently, several of the tryptophan residues evolve from an apolar to a polar environment in two separate steps during unfolding. From this representation of the data, the fluorescence contribution of each particular tryptophan indole could not be discerned.

In contrast, plots of denaturation curves from the intensities at 332 nm gave a pattern that was typical for each individual mutant (Figure 4). The plot of pwt displays two transitions of almost equal amplitude. For the mutants W5F and W209F, the first transition has a larger amplitude than the first transition of pwt, whereas the second transition seems unaffected since it is similar in size to the pwt second transition. The profiles of W16F and the double mutant W5F/W16F (data not shown) are almost superimposable but differ from both the pwt and W5F profiles, indicating interdependent fluorescence for tryptophans 5 and 16. In the region 1−1.5 M GuHCl, the mutants W16F, W5F/W16F, and W97C show a marked increase in fluorescence intensity, a feature that was also exhibited by pwt and W5F, although not so pronounced. This increase is probably caused by

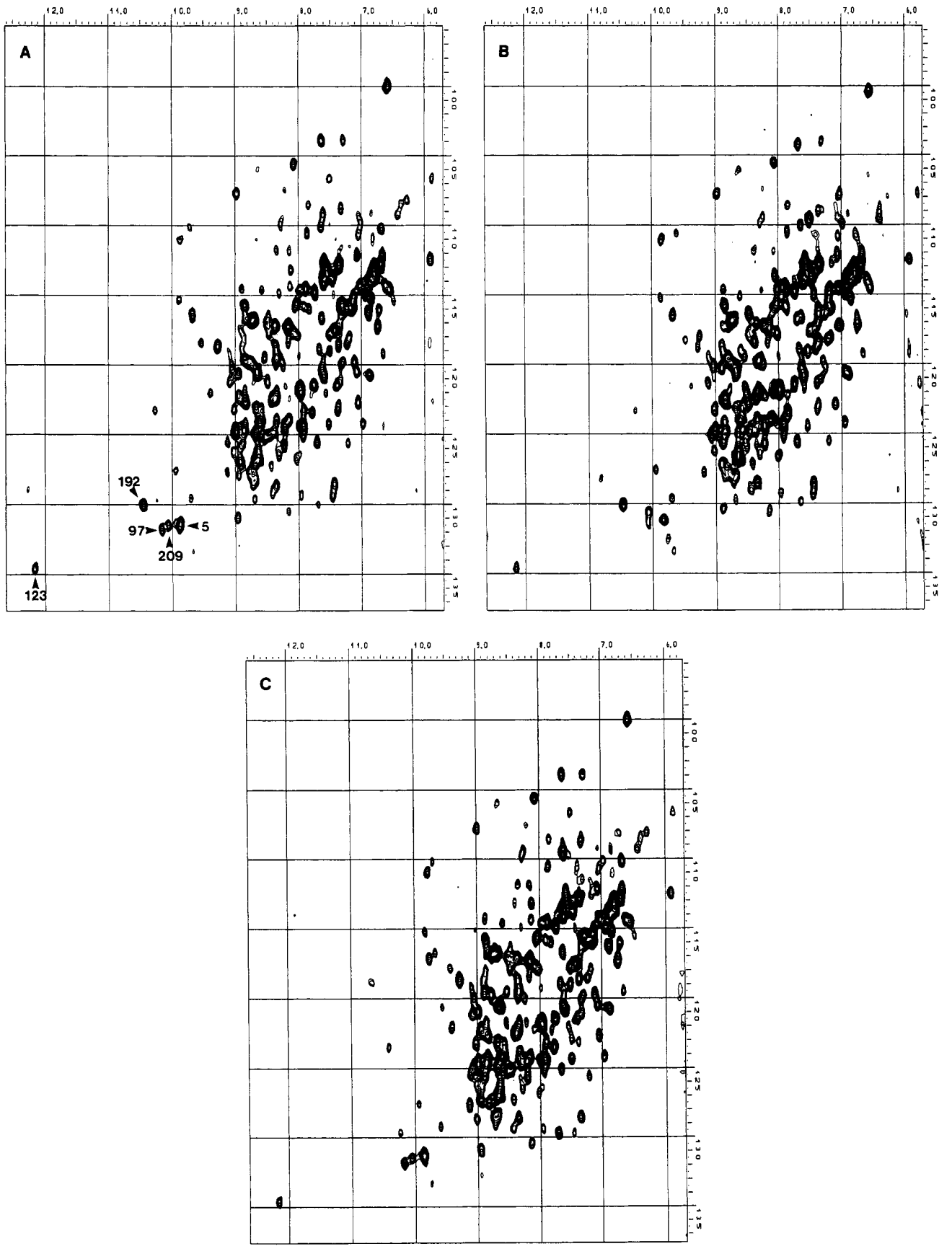

FIGURE 2: HSQC-NMR spectra of ^{15}N-labeled pwt (A), W97C (B), and W192F (C). Proton shifts are indicated on the horizontal axis, while the vertical axis shows ^{15}N shifts. The assignments of Trp indole NH groups are indicated in the pwt spectrum (A) by an arrow and the Trp number.

structural alterations that move internal quenchers from the vincinity of some of the tryptophans, i.e., leading to less quenching. These matters are discussed in more detail later.

The mutation W123C resulted in a curve with a dominating first transition and possibly a small second transition. In the case of W97C, which emitted much less light than any

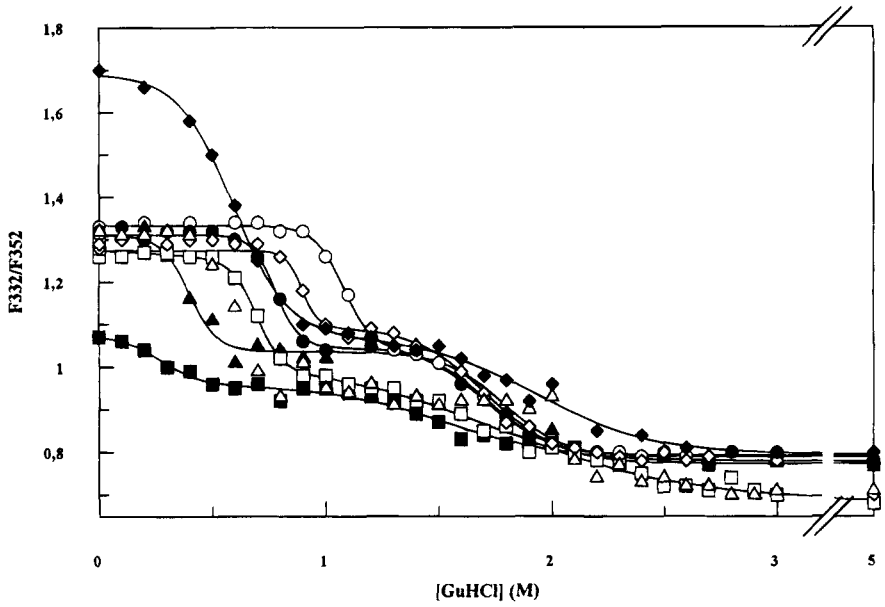

FIGURE 3: GuHCl denaturation of tryptophan mutants as monitored by intrinsic tryptophan fluorescence and presented as ratios between intensities at 332 and 352 nm (excitation at 295 nm). Symbols: pwt (○), W5F (●), W16F (▲), W97C (■), W123C (□), W192F (◇), W209F (△), W245C (◆).

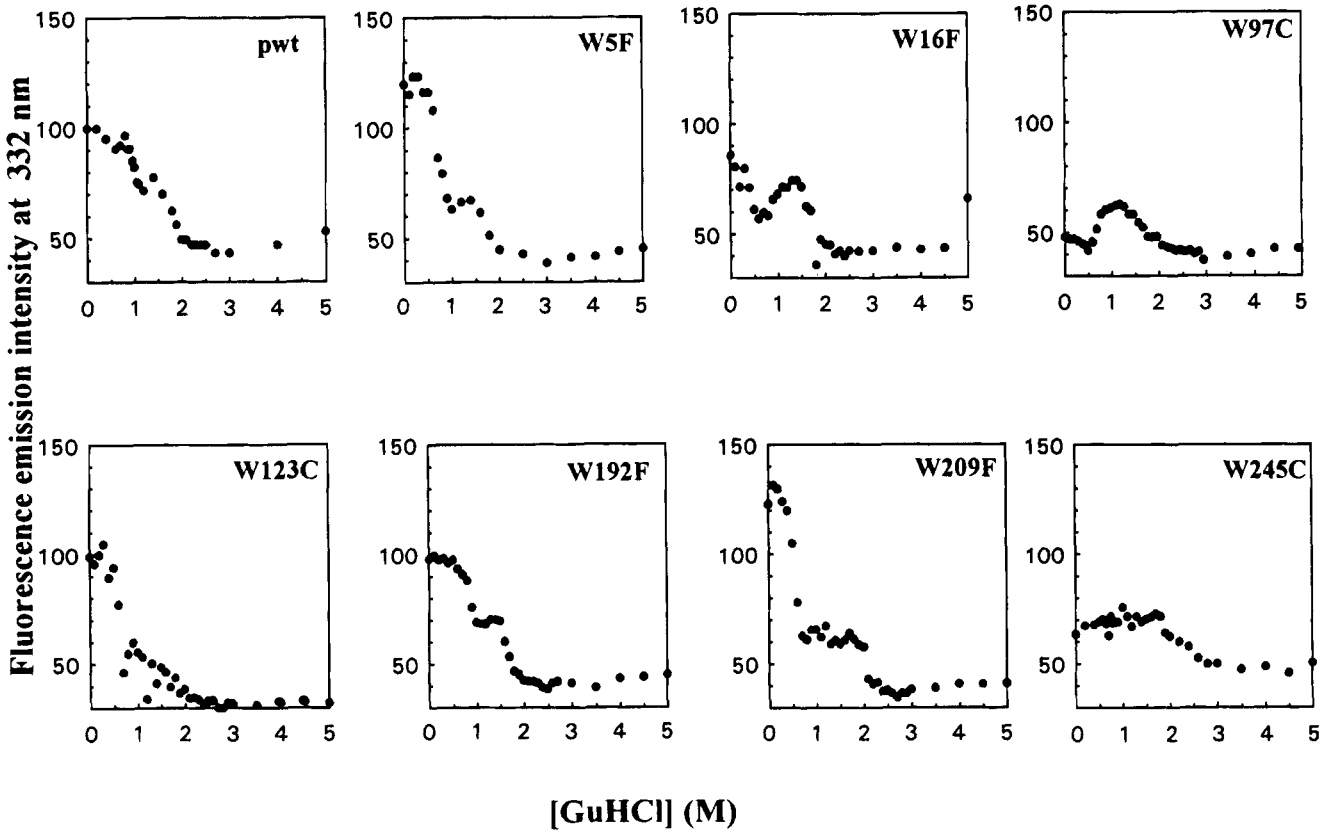

FIGURE 4: GuHCl denaturation of tryptophan mutants monitored by intrinsic tryptophan fluorescence at 332 nm (excitation at 295 nm). The intensity of each variant is normalized to pwt in 0 M GuHCl.

other mutant, denaturation in GuHCl caused only small changes in fluorescence intensity. The most striking feature of the W245C mutant is that only the second transition is reflected in the F_{332} denaturation curve. One explanation for this might be that Trp245 is responsible for much of the decrease in intensity in the first transition of pwt and other mutants than W245C. Interestingly, the F_{332}/F_{352} ratio shows a decrease in the first transition for the W245C mutant as well as for the other mutants, illustrating that the ratio is monitoring wavelength shifts rather than changes in intensities.

Relative Fluorescence Intensities. The complex denaturation curves that are shown in Figure 3 indicate that, after excitation, energy might migrate among tryptophans and that fluorescence from some tryptophans might be quenched by nearby amino acid residues. To further investigate this possibility, we carefully repeated our measurements of fluorescence intensity at three GuHCl concentrations (0, 1.5,

Table 2: Fluorescence Emission at pH 7.5 Measured as the Maximal Intensity for Each Mutant at Different GuHCl Concentrations

enzyme variant	relative intensity (%)		
	0 M GuHCl	1.5 M GuHCl	5 M GuHCl
pwt[a]	100 (332)	100 (343)	100 (352)
H64A	117 ± 3 (333)	106 ± 4 (342)	102 ± 5 (351)
W5F	119 ± 5 (333)	96 ± 4 (342)	91 ± 4 (352)
W5F/W16F	69 ± 4 (330)	78 ± 2 (338)	71 ± 5 (350)
W16F	85 ± 2 (332)	83 ± 3 (341)	82 ± 6 (351)
W97C	48 ± 5 (334)	77 ± 6 (344)	87 ± 5 (352)
W123C	98 ± 4 (333)	77 ± 6 (345)	82 ± 5 (351)
W192F	98 ± 4 (332)	88 ± 3 (341)	89 ± 4 (352)
W209F	123 ± 5 (332)	73 ± 6 (345)	79 ± 4 (351)
W245C	62 ± 4 (328)	92 ± 8 (340)	88 ± 6 (352)

[a] pwt was set as 100% at each GuHCl concentration. Values in parentheses are the emission wavelength maxima (nm), and the errors are standard deviations.

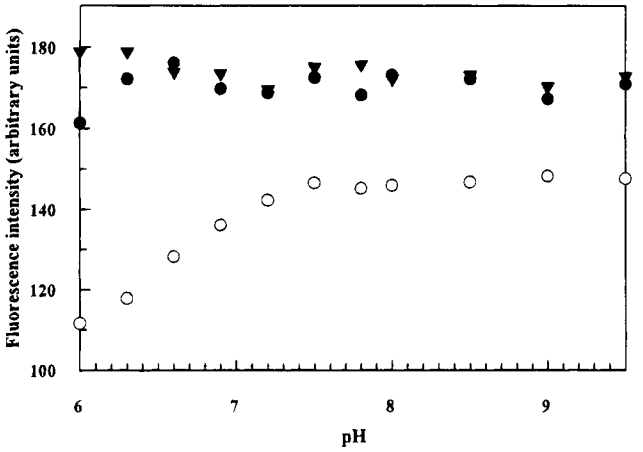

FIGURE 5: pH titration of pwt (○), W5F (●), and H64A (▼). The intensity of fluorescence emission of solutions of different pH values in a mixed buffer of Mes, Hepes, Taps, and Caps (50 mM each) containing 0.85 μM protein was recorded at 332 nm.

and 5 M GuHCl) corresponding to the native, intermediate, and unfolded states. The emission intensities were measured at the λ_{max} value of each mutant. To increase the accuracy, most experiments were repeated at least three times. The results summarized in Table 2 are mean values from these measurements. Considering 0 M GuHCl, it can be concluded that the major fluorescence emitters in the native state are Trp97 and Trp245, since removal of these residues causes a large decrease in fluorescence intensity. On the other hand, Trp5 and Trp209 make a negative contribution to the fluorescence intensity, i.e., the mutants lacking these tryptophans exhibit an increase in fluorescence when compared to the pwt.

To test whether the imidazole side chain of His64 might act as a quencher of Trp5 fluorescence, we measured the dependence of the fluorescence intensity on pH for a mutant where His64 is replaced by Ala (Figure 5, Table 2). Identical experiments were also done on the pwt and the W5F mutant, and they show that part of the pwt fluorescence is dependent on pH with an apparent pK_a around 7. The emissions from H64A and W5F are almost identical and show no dependence on pH in the region between 6 and 9.5. Replacement of Trp123 and Trp192 has virtually no effect on the fluorescence emission.

At the intermediate GuHCl concentration, the mutations lower the fluorescence intensity by 4% to 27%. Notably, the mutation of Trp5 lowers the emission intensity by only 4%. From the results at 5.0 M GuHCl, it seems as if each tryptophan contributes between 9% and 29% of the total intensity of the pwt.

Difference Spectra. The contribution from each individual tryptophan to the fluorescence spectrum may be difficult to discern by a visual inspection of the spectra of the mutants. Therefore, we have calculated difference spectra between the pwt spectrum and the spectrum of each Trp mutant. For tryptophans that are not involved in complex energy transfer reactions, this procedure will give a difference that represents the spectrum of the particular mutated tryptophan residue. A selection of such difference spectra, from measurements at 0 and 1.5 M GuHCl, is shown in Figures 8 and 9, respectively.

Quenching of Intrinsic Fluorescence by Acrylamide. Quenching of tryptophan fluorescence by the addition of acrylamide at 0, 1.5, and 5 M GuHCl was performed to investigate the exposure of the various tryptophans in the native, intermediate, and unfolded states, respectively. Stern–Volmer plots of the results are shown in Figure 6. A gradual increase in acrylamide quenching efficiency is seen for all mutants when going from 0 to 1.5 to 5 M GuHCl. However, by examining each mutation individually, they seem to be affected in distinct ways by the quencher at the different GuHCl concentrations.

DISCUSSION

The main purpose of this study was to investigate protein unfolding by use of the spectral properties of Trp residues. Studying fluorescence can provide information about energy transfer and quenching by neighboring groups. However, since HCA II has seven tryptophans, problems may arise while attempting to distinguish their individual emissions. This can be overcome by using the results of the present study, which allow the tryptophans in HCA II to be divided into four groups (Table 2): (i) those that affect the fluorescence intensity markedly, i.e., cause a 30–50% decrease in fluorescence intensity when replaced (Trp97 and Trp245); (ii) those that affect intensity as much as expected for a protein variant lacking one out of seven tryptophans (Trp16); (iii) those having hardly any effect at all on fluorescence intensity (Trp123 and Trp192); and (iv) those making a negative contribution to the fluorescence intensity (Trp5 and Trp209).

Fluorescence Intensity, Energy Migration, and Internal Quenching of Fluorescence. This section presents an interpretation of the results of the fluorescence intensity measurements for the different mutants in their native states (Figure 7).

W97C: Mutation of Trp97 to cysteine resulted in a spectrum with fluorescence intensity being only 48% of the pwt, which is the largest reduction we have observed. Thus, Trp97 must be the major fluorescence emitter, and there are no indications that this residue is involved in energy transfer or quenching.

W245C: Trp245 is the second major emitter since the mutation W245C lowered fluorescence intensity to 62%. None of our findings indicate that Trp245 is involved in energy transfer or quenching.

W123C: Mutation of Trp123 to cysteine in no way affected the fluorescence spectra, which may indicate that

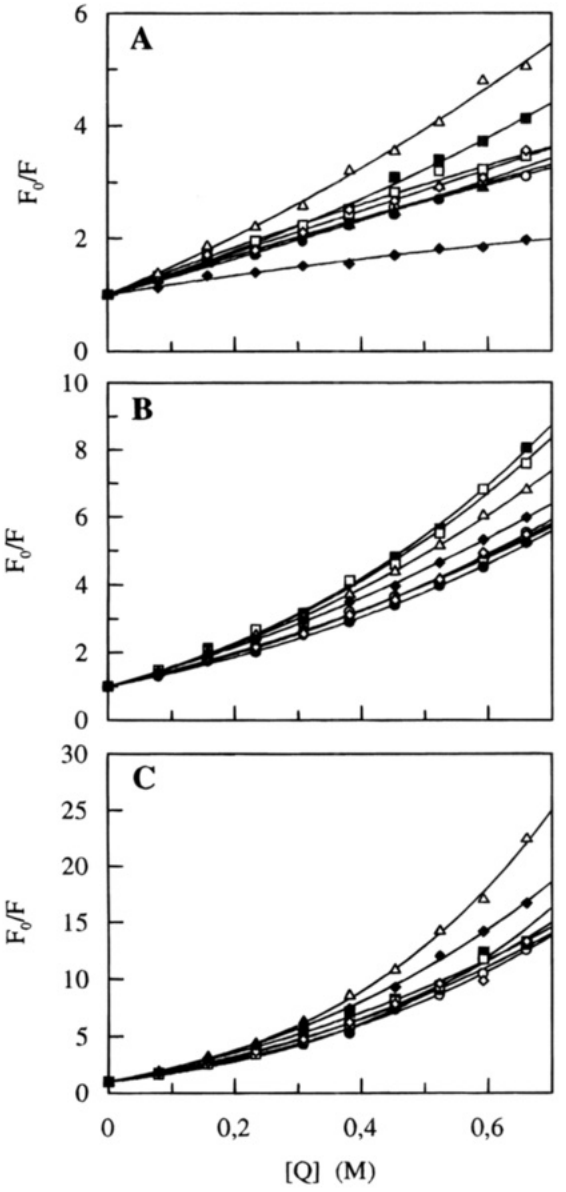

FIGURE 6: Stern−Volmer plots for the acrylamide quenching of the fluorescence of the different variants of HCA II incubated in 0 (A), 1.5 (B), and 5 M GuHCl (C). Symbols: pwt (○), W5F (●), W16F (▲), W97C (■), W123C (□), W192F (◇), W209F (△), W245 (◆).

the fluorescence was quenched at Trp123 or that all of its energy was transferred to another Trp residue, which in turn was totally quenched. We favor the former interpretation since Trp123 is located close to the side chain of Arg89, which may act as a quencher.

W209F: The mutation of Trp209 to Phe resulted in a substantial increase in fluorescence emission. Therefore, we propose that fluorescence from Trp209 was quenched efficiently by the nearby His107 and His119. Histidine in position 107 is buried deep in the protein; hence, it is difficult to determine its pK_a by ^{1}H NMR pH titration. His119 is one of the ligands to the catalytically important Zn^{2+} ion, forming a complex that may be well suited for charge transfer reactions. Furthermore, energy is transferred to Trp209 (because of the increase in fluorescence in W209F), and we suggest that this energy comes from Trp192 (see the following).

W192F: As was the case for Trp123, the replacement of Trp192 did not affect fluorescence intensity. Also, in this

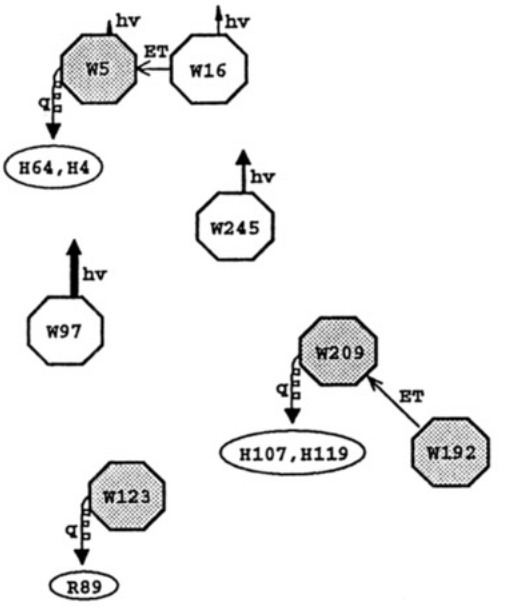

FIGURE 7: Cartoon to summarize the interpretation of fluorescence intensity data. Abbreviations: quenching, q; fluorescence emission, *hv*; energy transfer, ET. Putative quenching residues are encircled.

case there are two principal ways to interpret the data, and we favor the idea that energy is transferred from Trp192 to Trp209, which in turn is quenched. The reason for this is that we cannot find any potential quencher among the amino acid residues that are close to Trp192. The closest indole is Trp209, at a distance of 10 Å, and the energy is probably transferred to that residue.

W16F: Mutation of Trp16 to Phe led to a minor decrease in fluorescence intensity, indicating that part of the energy from Trp16 was transferred to the nearby Trp5 and the remaining energy was emitted as fluorescence. That the intensity was lower for the double mutant W5F/W16F than for the single mutant W16F might indicate that Trp5 normally loses some of its energy as fluorescence, implying that Trp5 is not fully quenched at this pH (see following section). Another possibility that must be considered, because Trp5 and Trp16 are close neighbors in the structure, is that they may be coupled via exciton coupling and therefore absorb and emit energy as a single unit.

W5F: Mutation of Trp5 to Phe led to an increase in fluorescence emission, indicating that Trp5 is quenched by neighboring amino acid side chains and also that energy is transferred to Trp5 from a nearby Trp. Analysis of the X-ray structure indicated that obvious candidates for quencher are His4 and His64, which are both within van der Waals contact distance of Trp5. To test this hypothesis, we measured the fluorescence from a mutant in which His64 had been replaced by an alanine residue. Interestingly, the H64A mutation also led to a considerable increase in fluorescence intensity similar to the effect of the W5F mutation, which strongly supports our hypothesis (Table 2, Figure 5). Since it is the protonated form of imidazole that is known to be an efficient quencher, and the present measurements were performed at pH 7.5, while the pK_a of His64 is 7.0 and that of His4 may be as low as 6.0, as determined by ^{1}H NMR pH titrations (Campbell et al., 1975), we measured the dependence of the quenching efficiency on pH. However, removal of all quenchers should result in a protein with higher fluorescence emission than the W5F mutant because the fluorescence from

the H64A mutant must contain contributions both from an unquenched Trp5 and from another Trp via energy transfer. Removal of Trp5 can, on the other hand, only lead to an increase in fluorescence intensity that corresponds to the energy that is transferred from another Trp. Hence, His4 may contribute somewhat to the quenching of Trp5 fluorescence. The most plausible candidate for donation of energy to Trp5 is Trp16: this residue is situated at van der Waals distance from Trp5 and in a position face to edge to the indole ring of Trp5.

Characterization of the Native, Intermediate, and Denatured States. The interpretations of the fluorescence intensities for the different mutants in their native states, as presented earlier and summarized in Figure 7, are used as a starting point for the following discussion in which all other results are included. The aim is to characterize the local structure around each tryptophan in the native, intermediate, and unfolded states. In the discussion of the data on the native state, the conclusions about structure are compared with the known 3-dimensional structure from X-ray analysis (Håkansson et al., 1992).

Native State. Calhoun et al. (1986) found that fluorescence from solvent-exposed Trp is more efficiently quenched by acrylamide than that from buried Trp, and from a comparison of quenching by O_2 and by acrylamide, they concluded that acrylamide does not readily penetrate native protein structures. One must note that, in the interpretation of acrylamide quenching data, we compare the quenching of pwt and a mutant with one less Trp. The difference in quenching efficiency then must reflect the accessibility of the removed Trp to acrylamide, i.e., removal of a buried Trp will lead to a mutant protein having fluorescence that is relatively more efficiently quenched. Stern−Volmer plots from our studies of native pwt and mutant proteins show that acrylamide quenches the fluorescence from the W97C and W209F mutants more efficiently than that of the pwt (Figure 6A).

Interpretation of the result of W97C is straightforward. Trp97 is the major emitter and it is buried deep in the protein interior; therefore, the mutation that removed Trp97 led to a protein with relatively more exposed tryptophans and, as a consequence, to relatively more efficient quenching. The difference spectra in Figure 8 show that the fluorescence spectrum from the particular Trp97, with an emission maximum at 335 nm, is blue-shifted when compared to the other observable spectra from individual tryptophans. Hence, the results indicate that Trp97 is situated in a mainly apolar environment, which is in accord with X-ray crystallography data. The efficient acrylamide quenching of the fluorescence from the W209F mutant cannot be explained in a manner similar to that for the W97C mutant because fluorescence intensity data show that Trp209 is already quenched in the native state by internal quenchers. Instead, the results support our interpretation of the fluorescence intensity data, which was that in the native pwt energy is transferred radiationless from Trp192 to Trp209. In the mutant W209F the acceptor Trp is removed, and therefore the energy from Trp192 is now emitted as fluorescence and thus relatively more fluorescence can be quenched by acrylamide in the W209F mutant than in the pwt. According to X-ray data, Trp192 is exposed to the surface by 13 Å^2 (Table 3), which probably reflects a static situation. Since the quenching efficiency is dependent on the dynamic accessibility, our results seem to indicate that Trp192 has significant dynamic accessibility as well.

Table 3: Solvent Accessible Surface Area for Individual Tryptophan Side Chains of HCA II

Trp residue	surface area (Å^2)[a]	fraction R[b]	fraction T[c]
5	22	0.10	0.23
16	4	0.02	0.04
97	0	0	0
123	6	0.03	0.06
192	13	0.06	0.14
209	4	0.02	0.04
245	47	0.22	0.49

[a] Solvent accessible surface area in angstroms for the specific Trp residue. [b] Fraction of solvent accessible surface area to side chain atom of a Trp residue. [c] Fraction of solvent accessible surface area to total solvent accessible surface area of the sum of Trp residues in HCA II. Accessible surface area of Trp in a Gly-Trp-Gly tripeptide in an extended conformation has been used in this calculation. The total solvent accessible surface area for the Trp side chain in this tripeptide is 217 Å^2 (Miller et al., 1987).

The second major fluorescence emitter is Trp245. Analysis of the difference fluorescence spectrum for the mutant W245C (Figure 8) indicates that the spectrum of the particular Trp245 is red-shifted when compared to spectra for the other tryptophans. These data go well with crystallographic data that show that Trp245 is by far the most solvent accessible of all the tryptophans. Consequently, in the W245C mutant most of the fluorescence is emitted from Trp97, which is buried deep in the protein, and therefore quenching of the fluorescence by acrylamide is not efficient (Figure 6A).

Intermediate State. Measurement of the fluorescence intensity of the pwt and mutant proteins, incubated in 1.5 M GuHCl, indicates that the intermediate state has no dominating fluorescence emitters. Summation of the contributions from each tryptophan adds up to 115% (Table 2), which indicates that energy transfer between tryptophans followed by internal quenching may also take place, but to a minor extent, in the intermediate state. Possible candidates are the Trp5−Trp16 couple, because mutation of Trp5 reduces the fluorescence intensity by only 4% and because the mutation of His64 to Ala increases the fluorescence yield to 106%. Since His64 was shown to quench the fluorescence from Trp5 in the native state, one may speculate that Trp5 and His64 also have frequent encounters in the intermediate state. However, the results on the mutants W97C, W123C, and W209F clearly are more comprehensible. First, we may note that, although not dominating, these residues have the largest contributions to the fluorescence spectrum. In the absence of extensive internal quenching, this may indicate that these residues are situated in relatively more apolar environments than other residues. Stronger support for this proposal can be found when analyzing the fluorescence difference spectra. At 1.5 M GuHCl the particular tryptophans 97, 123, and 209 have the most blue-shifted spectra, showing similar emission maxima (Figure 9, Table 4). Therefore, it seems as if the intermediate state contains a region, encompassing residues 97, 123, and 209, that is quite apolar. Among the other tryptophans, it seems as though Trp192 has only a slightly more polar environment than the discussed tryptophans, while the spectrum of Trp16 has an emission maximum that is as red-shifted as that measured at 5 M GuHCl. Hence, the N-terminal peptide segment, or at least the environment

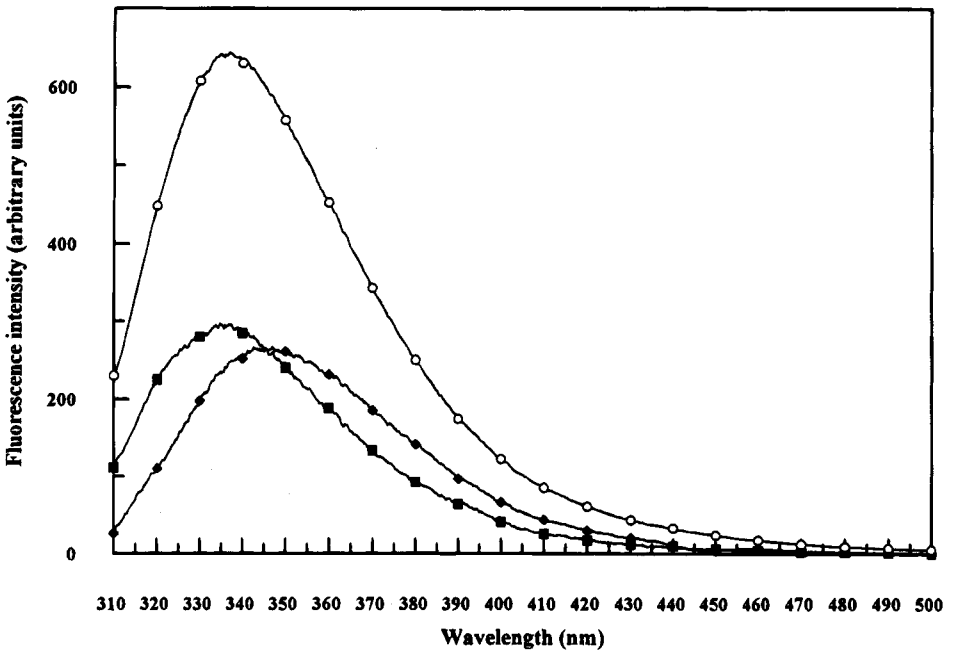

FIGURE 8: Fluorescence emission spectra at 0 M GuHCl of the individual Trp residues 97 (■) and 245 (◆) obtained as difference spectra (pwt − mutant). The spectrum of pwt (○) is included as a reference.

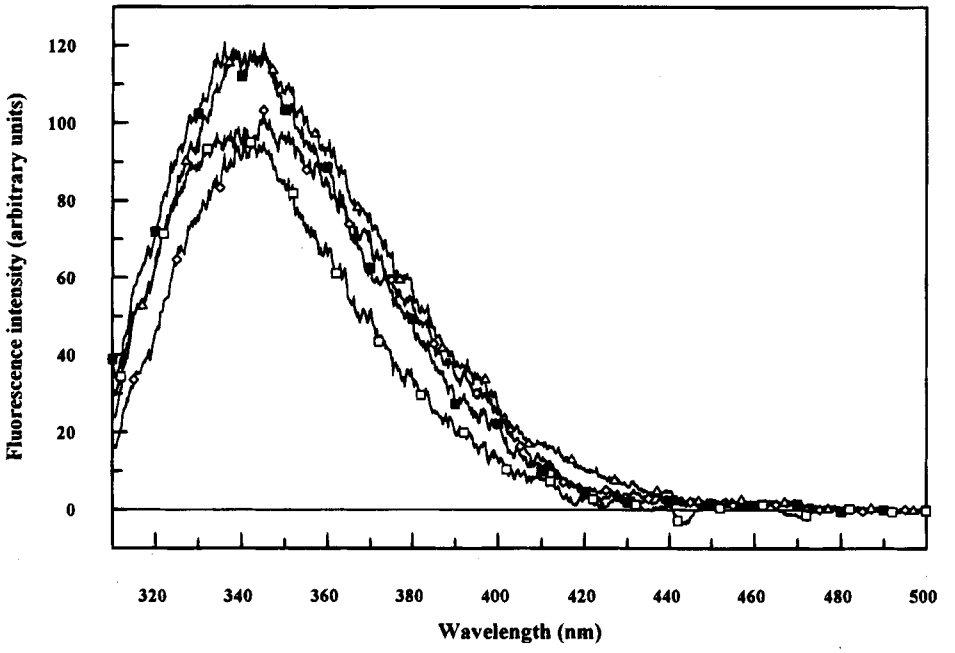

FIGURE 9: Difference fluorescence spectra (pwt − mutant) at 1.5 M GuHCl showing the individual contributions from Trp97 (■), Trp123 (□), Trp192 (◇), and Trp209 (△).

of Trp16, seems to be fully exposed to the solvent already in the intermediate state. The spectra of the pwt and W5F mutant are very similar, and therefore it was not possible to determine the particular spectrum for Trp5 from a calculation of the difference. Analysis of acrylamide quenching data gives a similar result, namely, that residues 97, 123, and 209 are relatively more shielded from external quenchers than any of the other residues (i.e., the fluorescence from mutants without these tryptophans is quenched more efficiently by acrylamide than the fluorescence from the pwt) (Figure 6B).

Unfolded State. At 5 M GuHCl, all tryptophans seem to be fully accessible to quenching of their fluorscence by acrylamide, with the exception of Trp209 (Figure 6C). Interestingly, analysis of the fluorescence spectra, from measurements on the mutant proteins in 5 M GuHCl, shows that Trp209 contributes slightly more than any of the other tryptophans to the fluorescence intensity. Hence, it is possible that the region around Trp209 is not completely unfolded at 5 M GuHCl.

CONCLUDING REMARKS

In this study, specific fluorescence properties were assigned to each tryptophan in the native structure of human carbonic anhydrase II. Acrylamide quenching of fluorescence led to a more detailed characterization of the intermediate state than was available previously. The results indicated that tryptophan residues 97, 123, and 209 are involved in a rather compact and hydrophobic structure in

Table 4: Wavelength Emission Maxima for the Particular Tryptophan Residues of HCA II at Different GuHCl Concentrations as Indicated by Difference Spectra

tryptophan residue	λ_{max} (nm)		
	0 M GuHCl	1.5 M GuHCl	5 M GuHCl
5	337[a]	[b]	355
16	341	355	356
97	335	340	355
123	[b]	340	353
192	[b]	344	354
209	333[a]	341	353
245	345	[b]	352

[a] The difference spectrum probably does not represent the particular Trp residue due to complex energy transfer reactions. [b] The peak had too low intensity to allow an accurate determination of λ_{max} (see Table 2).

the intermediate state. The native structure of HCAII is dominated by a 10-stranded β-structure that extends throughout the entire molecule (Håkansson et al., 1992). Recently, we reported studies that were aimed at mapping the molten globule intermediate structure by measuring the alkylation rates of purposely introduced SH groups (Mårtensson et al., 1993). These studies showed that the region around β-strands 9 and 10 was rather flexible in the intermediate state. The fluorescence spectrum of Trp192, which is situated in β-strand 8, indicates that the opening up of the structure extends to this position. Alkylation rates of an SH group in position 206, in β-strand 7, indicated that this β-strand was hidden in the intermediate state. This conclusion is supported by the observation that the fluorescence spectrum of Trp209, which is also situated in β-strand 7, is more blue-shifted than that of Trp192. Measurements of the alkylation of an SH group introduced at position 68 (β-strand 3) showed that this substructure was extremely compact and stable even at 5 M GuHCl. β-strand 4 probably is also in a very compact environment in the intermediate state, because Trp97, which is situated in β-strand 4 and is part of a large aromatic cluster, has one of the most blue-shifted spectra of all the tryptophans in the intermediate state.

ACKNOWLEDGMENT

We thank Ms. Katarina Wallgren for excellent technical assistance, Dr. Ingmar Sethson for recording the NMR spectra, and Professor Anders Liljas for providing data for Table 3.

REFERENCES

Banik, U., Saha, R., Mandal, N. C., Bhattacharyya, B., & Roy, S. (1992) *Eur. J. Biochem. 206*, 15−21.

Bodenhausen, G., & Ruben, D. J. (1980) *Chem. Phys. Lett. 69*, 185.

Calhoun, B. D., Vanderkooi, J. M., Holtom, G. R., & Englander, S. W. (1986) *Proteins: Struct. Funct. Genet. 1*, 109−115.

Campbell, I. D., Lindskog, S., & White, A. I. (1975) *J. Mol. Biol. 98*, 597−614.

Carlsson, U., Henderson, L. E., & Lindskog, S. (1973) *Biochim. Biophys. Acta 310*, 376−387.

Edsall, J. T., Mehta, S., Myers, D. V., & Armstrong, J. M. (1966) *Biochem. Z. 345*, 9−36.

Eftink, M. R., & Ghiron, C. A. (1976) *J. Phys. Chem. 80*, 486−493.

Freskgård, P.-O., Mårtensson, L.-G., Jonasson, P., Jonsson, B.-H., & Carlsson, U. (1994) *Biochemistry 33*, 14281−14288.

Garvey, E. P., & Matthews, C. R. (1989) *Biochemistry 28*, 2083−2093.

Gill, S. C., & von Hippel, P. H. (1989) *Anal. Biochem. 182*, 319−326.

Hemsley, A., Arnheim, N., Toney, M. D., Cortopassi, G., & Galas, D. J. (1989) *Nucleic Acids Res. 17*, 6545−6551.

Henderson, L. E., Henriksson, D., & Nyman, P. O. (1976) *J. Biol. Chem. 251*, 5457−5463.

Henkens, R. W., Kitchell, B. B., Lottich, S. C., Stein, P. J., & Williams T. J. (1982) *Biochemistry 21*, 5918−5923.

Hewett-Emmet, D., Hopkins, P. J., Tashian, R. E., & Czelusniak, J. (1984) *Ann. N. Y. Acad. Sci. 429*, 338−358.

Håkansson, K., Carlsson, M., Svensson, L. A., & Liljas, A. (1992) *J. Mol. Biol. 227*, 1192−1204.

Khalifah, R. G., Strader, D. J., Bryant, S. H., & Gibbons, S. M. (1977) *Biochemistry 28*, 4914−4922.

Kunkel, T. A. (1985) *Proc. Natl. Acad. Sci. U.S.A. 82*, 488−492.

Loewenthal, R., Sancho, J., & Fersht, A. R. (1991) *Biochemistry 30*, 6775−6779.

Mårtensson, L.-G., Jonsson, B.-H., Andersson, M., Kihlgren, A., Bergenhem, N., & Carlsson, U. (1992) *Biochim. Biophys. Acta 1118*, 179−186.

Mårtensson, L.-G., Jonsson, B.-H., Freskgård, P.-O., Kihlgren, A., Svensson, M., & Carlsson, U. (1993) *Biochemistry 32*, 224−231.

McCoy, L. F., Rowe, E. S., & Wong, K.-P. (1980) *Biochemistry 19*, 4738−4743.

Miller, S., Janin, J., Lesk, A. M., & Chothia, C. (1987) *J. Mol. Biol. 196*, 641−656.

Nair, S. K., Calderone, T. L., Christianson, D. W., & Fierke, C. A. (1991) *J. Biol. Chem. 266*, 17320−17325.

Nozaki, Y. (1972) *Methods Enzymol. 26*, 43−50.

Nyman, P. O., & Lindskog, S. (1964) *Biochim. Biophys. Acta 85*, 141−151.

Sanger, F., Nicklen, S., & Coulson, A. R. (1977) *Proc. Natl. Acad. Sci. U.S.A. 74*, 5457−5463.

Smith, J. C., Clarke, A. R., Chia, W. N., Irons, L. I., Atkinson, T., & Holbrook, J. J. (1991) *Biochemistry 30*, 1028−1036.

Studier, F. W., & Moffatt, B. A. (1986) *J. Mol. Biol. 189*, 113−130.

BI941010D